



Effects of ocean acidification with $p\text{CO}_2$ diurnal fluctuations on survival and larval shell formation of Ezo abalone, *Haliotis discus hannai*

Toshihiro Onitsuka^{a,*}, Hideki Takami^b, Daisuke Muraoka^c, Yukio Matsumoto^c,
Ayumi Nakatsubo^d, Ryo Kimura^e, Tsuneo Ono^f, Yukihiro Nojiri^g

^a Kushiro Laboratory, Hokkaido National Fisheries Research Institute, Japan Fisheries Research and Education Agency, 116 Katsurakoi, Kushiro, Hokkaido 085-0802, Japan

^b Tohoku National Fisheries Research Institute, Japan Fisheries Research and Education Agency, 3-27-5 Shinhamma, Shiogama, Miyagi 985-0001, Japan

^c Miyako Laboratory, Tohoku National Fisheries Research Institute, Japan Fisheries Research and Education Agency, 4-9-1 Sakiyama, Miyako, Iwate 027-0097, Japan

^d Faculty of Agriculture, Yamagata University, 5-3 Takasaka, Tsuruoka, Yamagata 997-0369, Japan

^e Japan Fisheries Research and Education Agency, 2-12-4 Fukuura, Kanazawa-ku, Yokohama, Kanagawa 236-8648, Japan

^f Yokohama Laboratory, National Research Institute of Far Seas Fisheries, Japan Fisheries Research and Education Agency, 2-12-4 Fukuura, Kanazawa-ku, Yokohama, Kanagawa 236-8648, Japan

^g Department of Earth and Environmental Sciences, Hirosaki University, 3 Bunkyocho, Hirosaki, Aomori 036-8560, Japan

ARTICLE INFO

Keywords:

Climate change
Gastropods
Diel fluctuation
Periodic $p\text{CO}_2$ amplitude
pH
Larval shell
Survival

ABSTRACT

This study assessed the effects of constant and diurnally fluctuating $p\text{CO}_2$ on development and shell formation of larval abalone *Haliotis discus hannai*. The larvae was exposed to different $p\text{CO}_2$ conditions; constant [450, 800, or 1200 μatm in the first experiment (Exp. I), 450 or 780 μatm in the second experiment (Exp. II)] or diurnally fluctuating $p\text{CO}_2$ (800 \pm 400 or 1200 \pm 400 μatm in Exp. I, 450 \pm 80, 780 \pm 200 or 780 \pm 400 μatm in Exp. II). Mortality, malformation rates or shell length of larval abalone were not significantly different among the 450, 800, and 800 \pm 400 μatm $p\text{CO}_2$ treatments. Meanwhile, significantly higher malformation rates and smaller shells were detected in the 1200 and 1200 \pm 400 μatm $p\text{CO}_2$ treatments than in the 450 μatm $p\text{CO}_2$ treatment. The negative impacts were greater in the 1200 \pm 400 μatm than in the 1200 μatm . Shell length and malformation rate of larval abalone were related with aragonite saturation state (Ω -aragonite) in experimental seawater, and greatly changed around 1.1 of Ω -aragonite which corresponded to 1000–1300 μatm $p\text{CO}_2$. These results indicate that there is a $p\text{CO}_2$ threshold associated with Ω -aragonite in the seawater, and that $p\text{CO}_2$ fluctuations produce additional negative impacts on abalone when above the threshold. Clear relationships were detected between abalone fitness and the integrated $p\text{CO}_2$ value over the threshold, indicating that the effects of OA on development and shell formation of larval abalone can be determined by intensity and time of exposure to $p\text{CO}_2$ over the threshold.

1. Introduction

Ocean acidification (OA) is the process of sustained absorption of anthropogenic carbon dioxide (CO_2) by the ocean (Caldeira and Wickett, 2003) that has been progressing rapidly since the Industrial Revolution. Elevated partial pressure of CO_2 ($p\text{CO}_2$) in seawater reduces pH (Caldeira and Wickett, 2003) and carbonate ion (CO_3^{2-}) availability (Gattuso and Buddemeier, 2000; Feely et al., 2004; Gazeau et al., 2007; Kurihara, 2008) and, consequently, significantly affects marine organisms and ecosystems. Most marine organisms with calcium carbonate (CaCO_3) skeletons or shells, such as mollusks, crustaceans, and echinoderms, are particularly susceptible to OA because the reduced pH and carbonate ion availability in seawater generally decrease the

calcification rate and/or increase dissolution of CaCO_3 structures (e.g., Riebesell et al., 2000; Feely et al., 2004). Moreover, physiological activities of marine animals, such as cellular functions and calcification, are mediated by disturbances and compensatory adjustments in acid–base status (e.g., Pörtner, 2008, 2012; Wittmann and Pörtner, 2013). Thus, it is believed that increasing CO_2 in ambient seawater due to progressive OA depresses metabolism and physiological activities by disturbing acid–base status and differential acid–base regulation within various body fluid compartments (Pörtner, 2012; Wittmann and Pörtner, 2013).

Many benthic invertebrates in coastal areas, including calcified organisms (calcifiers) are directly used by humans as fishery resources, and they play important roles in energy/nutrient flow and ecosystem

* Corresponding author.

E-mail address: onitsuka@affrc.go.jp (T. Onitsuka).

functioning. Most marine invertebrates are poikilosmotic animals with low capacity to regulate acid–base balance and have less osmoregulatory ability compared with those of vertebrate animals (Kokubo, 1962); thus, they are vulnerable to rapid increases in anthropogenic CO_2 , particularly during early life stages when internal physiological control is developing. Some groups of calcifiers, such as echinoderms, gastropods, and bivalves, show lower survival (Talmage and Gobler, 2009, 2011; Van Colen et al., 2012), retarded growth (Michaelidis et al., 2005; Shirayama and Thornton, 2005; Talmage and Gobler, 2011), and downsizing/malformation of the shell and skeletogenesis (Parker et al., 2009; Talmage and Gobler, 2009; Sheppard Brennan et al., 2010; Byrne et al., 2011; Kimura et al., 2011; Doo et al., 2012; Van Colen et al., 2012; Onitsuka et al., 2014; Tahil and Dy, 2016) in response to elevated seawater $p\text{CO}_2$. In contrast, several animals have nonlinear, neutral, or even positive reactions to elevated $p\text{CO}_2$ (e.g. Ries et al., 2009). Ultimately, the effects of increasing CO_2 in seawater likely vary among phyla, species, growth stage, latitude, and habitat (e.g. Watson et al., 2012).

The actual responses of animals to OA may be more complex under a natural environment including various biological and physicochemical phenomena. Seawater $p\text{CO}_2$ (pH) fluctuates diurnally in the ocean (Borges and Frankignoulle, 1999; Delille et al., 2009; Buapet et al., 2013; Cornwall et al., 2013; Onitsuka et al., 2014), which is generally driven by primary producers decreasing $p\text{CO}_2$ (increasing pH) in seawater during the day via photosynthesis and increasing $p\text{CO}_2$ (decreasing pH) at night via respiration (Buapet et al., 2013). For example, photosynthesis and respiration by macroalgae in kelp beds lead to marked $p\text{CO}_2$ diurnal fluctuations (Delille et al., 2009), which are larger than the $p\text{CO}_2$ change projected for open ocean waters due to OA by 2100 (Cornwall et al., 2013). However, most experimental studies that have examined the effects of OA on marine organisms have manipulated seawater $p\text{CO}_2$ or pH to a steady level predicted for the future. These studies have increased the understanding of how organisms respond to OA, but may have overlooked the importance of natural fluctuations in seawater $p\text{CO}_2$ on organismal response. Some studies have reported that diurnal variations in seawater $p\text{CO}_2$ affect the responses of marine animals to elevated $p\text{CO}_2$ (Clark and Gobler, 2016; Jarrold et al., 2017). Clark and Gobler (2016) showed that acidified and/or hypoxia condition produced reduced survival, slowed growth and delayed development of larval bivalves, and then diurnal fluctuation of the pH and/or dissolved oxygen (DO) did not fully mitigate the negative effects of hypoxia and/or acidification on the larvae. In contrast, Jarrold et al. (2017) demonstrated that diurnal $p\text{CO}_2$ cycles can substantially reduce the severity of behavioral abnormalities in coral reef fish caused by elevated seawater $p\text{CO}_2$. These results suggest that the responses of marine animals to increased and/or diurnal fluctuations in $p\text{CO}_2$ are highly species-specific. No information is available on how diurnal fluctuating $p\text{CO}_2$ affect the performance of most marine animals or how these fluctuations affect the responses of animals to increases in $p\text{CO}_2$ level due to progressive OA. Thus, incorporating the diurnal $p\text{CO}_2$ fluctuations that occur in the natural environment into OA-simulation experiments will help us better understand the changes in marine organisms and communities in an acidified ocean.

The objective of this study was to investigate the effects of OA in relation to diurnal cycles of $p\text{CO}_2$ on early life stages of Ezo abalone, *Haliotis discus hannai*. Abalone are an important coastal fishery resource worldwide and a target aquaculture species, and are also dominant grazers with relatively high biomass in coastal rocky reefs and exert great influences on food-web structures, energy/nutrient flow, and functioning of coastal ecosystems. Thus, understanding how abalone respond to increases and diurnal fluctuations in seawater $p\text{CO}_2$ will provide clues about changes in other benthic invertebrates and ecosystem structure/function in coastal rocky reefs, as well as the prospects for sustainability of natural abalone stocks. Some previous studies that evaluated the effects of OA on abalone species under static $p\text{CO}_2$ (pH) conditions reported that elevated $p\text{CO}_2$ seawater negatively affects

fertilization rate (Kimura et al., 2011), embryogenesis and hatching rate (Kimura et al., 2011; Tahil and Dy, 2016), survival (Crim et al., 2011; Kimura et al., 2011; Tahil and Dy, 2016), and larval shell morphology (Byrne et al., 2011; Crim et al., 2011; Kimura et al., 2011), compared with those in abalone species held in ambient natural seawater. Kimura et al. (2011) showed that static $p\text{CO}_2$ seawater < 1100 μatm (pH > 7.68) has no significant negative effect on fertilization, development, survival, or larval shell size of *H. discus hannai*, whereas highly-elevated $p\text{CO}_2$ [1650 (pH 7.49) and 2150 μatm $p\text{CO}_2$ (pH 7.41)] has adverse effects. These results suggest that there is a threshold level of $p\text{CO}_2$ between 1100 and 1650 μatm in which the early life stages of *H. discus hannai* are seriously affected. In natural habitats, *H. discus hannai* are generally competent to settle within a few days after fertilization, and then most larvae settled promptly on coastal reefs within a week after fertilization (Takami et al., 2006). Thus, diurnal fluctuations of $p\text{CO}_2$ in the coastal water can have considerable effect on abalone in early life. In this study, we focused on the period in the formation of larval shell, which will be particularly susceptible to reduced pH and carbonate ion availability in seawater by OA (e.g. Riebesell et al., 2000; Feely et al., 2004). To determine whether there is the threshold $p\text{CO}_2$ level in seawater that causes severe deterioration in early development and shell formation of abalone and how diurnal fluctuating $p\text{CO}_2$ interact with the responses of larval abalone to constant $p\text{CO}_2$ conditions, we reared larval abalone *H. discus hannai* under a series of constant and diurnally fluctuated $p\text{CO}_2$ treatments in the two different experiments. The aim of the first experiment was to determine how mean level and/or diurnal fluctuations of seawater $p\text{CO}_2$ affect early development and shell formation of larval abalone. If seawater TCO_2 balance in a day through photosynthesis/respiration of organisms were similar in future, magnitude of diurnally fluctuating $p\text{CO}_2$ become larger with increasing of mean $p\text{CO}_2$ level. Thus, the second experiment aimed how magnitude of diel $p\text{CO}_2$ cycles, which were designed based on TCO_2 scale, affect to the abalone performance.

2. Materials and methods

2.1. Rearing apparatus

Experiments were conducted at two onshore laboratories located at the Ezo abalone habitats in Shiogama and Miyako cities (Fig. S1, Table 1). Seawater was pumped from a subtidal intake situated near the laboratories, filtered through a cartridge filter (0.5- μm mesh), and pumped into a 150-L tank. The seawater temperature was controlled at $\sim 20^\circ\text{C}$ just before introduction into the CO_2 manipulation system. The effects of diurnal fluctuations in seawater $p\text{CO}_2$ on larval abalone malformation and mortality rates as well as shell length were examined using a highly accurate AICAL CO_2 manipulation system (e.g. Fujita et al., 2011; Kimura et al., 2011; Suwa et al., 2013; Onitsuka et al., 2014). This system consists of five parallel seawater manipulation lines that provide seawater controlled at a constant $p\text{CO}_2$ level or cyclically fluctuating $p\text{CO}_2$ levels. The system monitors the $p\text{CO}_2$ level in individual seawater lines. Seawater flows through a $p\text{CO}_2$ equilibration tower, which facilitates effective dissolution of gaseous CO_2 into the seawater, and continuously logs the seawater $p\text{CO}_2$ level, and the water is stored in a 5.5-L reservoir (Fig. 1). Then, the $p\text{CO}_2$ -conditioned seawater is distributed to each experimental chamber by a metering pump from the 5.5-L reservoir. The rearing system, including the AICAL system, which is the same as that used by Kimura et al. (2011) and Onitsuka et al. (2014), was used for all experiments in this study (Fig. 1).

2.2. Abalone rearing

Adult abalone, *H. discus hannai*, were collected on the subtidal rocky shore of the Sanriku coast, Japan (Fig. S1). The abalone were reared in tanks containing running sand-filtered seawater before induced

Table 1
Details on the rearing conditions and status of abalone used in the flowing water experiments (Exps. I and II).

Exp. no.	pCO ₂ treatment	Developmental stage of abalone at the beginning of Exp.	Initial status for larval shell	Rearing Temperature (°C)	Duration of experiment (days)	Number of replicate chamber	Number of abalone per chamber	Cohort of abalone	Experimental site
I	450 (AB)	Trochophore	unformed	20	3	3	200	2010	Shiogama
	800	Trochophore	unformed	20	3	3	200	2010	Shiogama
	800 ± 400	Trochophore	unformed	20	3	3	200	2010	Shiogama
	1200	Trochophore	unformed	20	3	3	200	2010	Shiogama
	1200 ± 400	Trochophore	unformed	20	3	3	200	2010	Shiogama
II	450 (AB)	Trochophore	unformed	20	3	5	200	2014	Miyako
	450 ± 80	Trochophore	unformed	20	3	5	200	2014	Miyako
	780	Trochophore	unformed	20	3	5	200	2014	Miyako
	780 ± 200	Trochophore	unformed	20	3	5	200	2014	Miyako
	780 ± 400	Trochophore	unformed	20	3	5	200	2014	Miyako

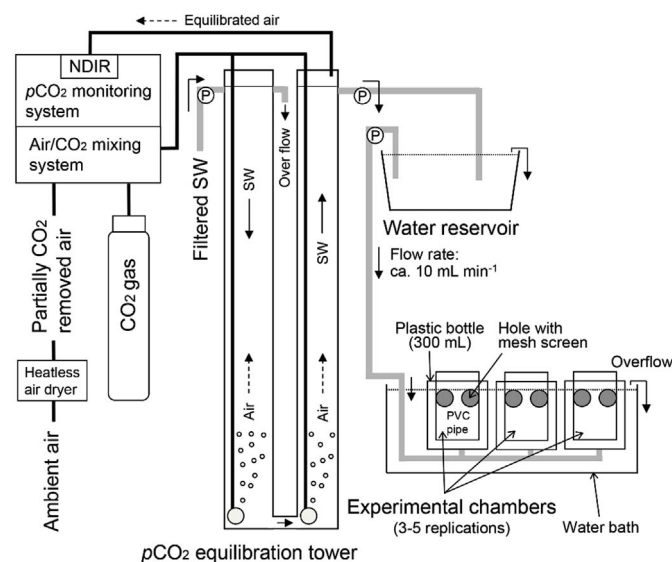


Fig. 1. Schematic figure of the pCO₂-control system and experimental chamber used in this study. Arrows show the direction of water or air flow. SW: seawater, NDIR: non-dispersive infrared gas analyzer, P: peristaltic pump.

spawning. Gonadal maturation was accelerated artificially by maintaining the animals in 20 °C seawater for several months. Five females and five males of abalone with fully mature gonads were selected and induced to spawn using UV-irradiated seawater (Uki and Kikuchi, 1984) on 20 December 2010 at the Shiogama laboratory and on 17 November 2014 at the Miyako laboratory (Table 1). Eggs and sperm obtained from the adults were kept separately in 20 °C UV-irradiated seawater for ~2 h prior to initiating the experiments.

2.3. Seawater pCO₂ experimental treatments

The pCO₂ of the experimental seawater was adjusted to a constant level or to diurnal fluctuating levels of pCO₂ as the first experimental condition (Table 1). Kimura et al. (2011) reported that constant pCO₂ seawater < 1100 μatm has no negative effect on fertilization, malformation, or mortality rates or larval shell formation of *H. discus hannai*. Thus, we used constant pCO₂ treatments that were lower (800 μatm) and higher (1200 μatm) than 1100 μatm pCO₂ (Table 1). The pCO₂ cyclical fluctuations involved changes of ± 400 μatm to the 800 and 1200 μatm treatments (800 ± 400 μatm pCO₂ and 1200 ± 400 μatm pCO₂ treatments, Table 1). Atmosphere-balanced pCO₂ seawater (~450 μatm) was used as a control. Target pCO₂ values of each treatment were set on the AICAL system as described in Table S1. This pCO₂-conditioned seawater was used in the Exp. I.

The second experimental condition involved experimental seawater

controlled to a constant or diurnal fluctuating pCO₂ level in the present and expected in the near future. We used 450 (atmosphere-balanced seawater; present level) and 780 μatm pCO₂ (near future level) as the constant pCO₂ treatments (Table 1). For the pCO₂-fluctuating treatments, fluctuation ranges of pCO₂ were given based on TCO₂ scale under the assumption that TCO₂ balance in a day through photosynthesis and respiration of organisms in near future were similar or greater than in the present. The pCO₂ values were determined beforehand from results of calculations with a target TCO₂ value under an average water quality conditions in the area (salinity, 34‰; temperature, 20 °C; and total alkalinity, 2231 μmol kg⁻¹) using the CO2SYS computer program (Pierrot et al., 2006). Under the water quality conditions, amount of change in pCO₂ per μmol kg⁻¹ TCO₂ became larger with increasing of pCO₂ level in the seawater. Consequently, the cyclically fluctuated pCO₂ treatments were prepared by adding ± ~80 μatm pCO₂ (corresponding to ± 50 μmol kg⁻¹ TCO₂) to the 450 μatm pCO₂ treatment as the present level, and adding ± ~200 μatm (± 50 μmol kg⁻¹ TCO₂; similar fluctuation in TCO₂ basis to the present) and ± ~400 μatm pCO₂ (± 80 μmol kg⁻¹ TCO₂; greater fluctuation in TCO₂ basis than the present) to the 780 μatm pCO₂ treatments as the near future level, respectively (Table 1). The target pCO₂ values of each treatment were set on the AICAL system as described in Table S1. The pCO₂-conditioned seawater was used in the Exp. II.

The pCO₂ fluctuation treatments in Exps. I and II involved a constant fluctuation range based on pCO₂ corresponding to pH change within 0.5 units (Table 2), which is reasonable for the pH variability in natural seaweed habitats as reported by Cornwall et al. (2013): pH variability within *Macrocystis pyrifera* kelp bed over 5 days in summer ranged by 0.94 units (Cornwall et al., 2013).

2.4. Rearing experiments

The first and the second experiments (Exps. I and II) were conducted to assess the effects of constant and diurnally fluctuating pCO₂ on mortality and malformation rates, as well as shell size of larval *H. discus hannai*.

Exp. I was conducted at the Shiogama laboratory during 20–24 December 2010 (Table 1). Gametes were fertilized in 20 °C UV-irradiated seawater and rinsed three times to remove excess sperm. The fertilized eggs were put in a 2-L plastic bottle containing 450 (atmosphere-balanced), 800, or 1200 μatm pCO₂ experimental seawater and kept in an incubation room at 20 °C. After the incubation, active and normally developed trochophore larvae with unformed shell were selected under a stereoscopic microscope and placed in the experimental chambers with running seawater adjusted to constant levels of 450 (atmosphere balanced seawater), 800, or 1200 μatm pCO₂ or fluctuating diel cycles (800 ± 400 and 1200 ± 400 μatm pCO₂ treatments) of pCO₂ at a density of 200 individuals per chamber (Table 1). Three experimental chambers were assigned to each pCO₂ treatment as

Table 2

Experimental conditions used in the flowing water experiments (Exps. I and II).

Exp. no.	pCO ₂ treatment	Measured pCO ₂ ^a (μatm)	Temperature ^a (°C)	Salinity (‰)	TA (μmol kg ⁻¹)	pH _{SWS} ^a	Ω _{calcite} ^a	Ω _{aragonite} ^a
I	450 (AB)	430.5 ± 15.1	20.1 ± 0.9	31	2106.2 ^c	7.99 ± 0.01	3.5 ± 0.1	2.3 ± 0.1
	800	721.3 ± 19.5	20.5 ± 0.6	31	2106.2 ^c	7.79 ± 0.01	2.4 ± 0.1	1.6 ± 0.1
	800 ± 400	788.2 ± 232.3	20.7 ± 0.7	31	2106.2 ^c	7.77 ± 0.12	2.4 ± 0.6	1.6 ± 0.4
		420.3–1189.0 ^b	–	–	–	7.60–8.00 ^b	1.6–3.7 ^b	1.0–2.4 ^b
	1200	1175.3 ± 19.6	20.5 ± 0.6	31	2106.2 ^c	7.60 ± 0.01	1.6 ± 0.1	1.0 ± 0.1
	1200 ± 400	1122.5 ± 251.9	20.1 ± 0.9	31	2106.2 ^c	7.63 ± 0.09	1.7 ± 0.3	1.1 ± 0.2
II		707.1–1537.1 ^b	–	–	–	7.49–7.80 ^b	1.3–2.3 ^b	0.8–1.6 ^b
	450 (AB)	450.8 ± 10.7	19.4 ± 0.6	33.9	2214.6	7.98 ± 0.01	3.7 ± 0.1	2.4 ± 0.1
	450 ± 80	483.9 ± 49.7	19.0 ± 0.7	33.9	2214.6	7.96 ± 0.04	3.5 ± 0.3	2.3 ± 0.2
		409.3–573.6 ^b	–	–	–	7.89–8.02 ^b	3.1–3.9 ^b	2.0–2.5 ^b
	780	719.5 ± 14.5	18.9 ± 0.7	33.9	2214.6	7.80 ± 0.01	2.6 ± 0.1	1.7 ± 0.1
	780 ± 200	779.6 ± 145.7	19.3 ± 0.5	33.9	2214.6	7.78 ± 0.07	2.5 ± 0.4	1.6 ± 0.2
		583.8–1035.0 ^b	–	–	–	7.66–7.88 ^b	1.9–3.1 ^b	1.3–2.0 ^b
	780 ± 400	780.6 ± 235.4	19.8 ± 0.5	33.9	2214.6	7.79 ± 0.11	2.6 ± 0.6	1.7 ± 0.4
		490.6–1243.9 ^b	–	–	–	7.59–7.95 ^b	1.7–3.5 ^b	1.1–2.3 ^b

^a Value of the parameter in the flowing water condition was shown as mean value ± standard deviation.^b A range of values for each parameter in the pCO₂ fluctuation treatments.^c An averaged value of TA data described in Table 1 of Kimura et al. (2011) was used as a TA value in this study.pH and carbonate saturation (Ω-calcite and Ω-aragonite) were calculated from the measured values of pCO₂, temperature, salinity and the TA value using 'CO₂SYS' software (see text). TA, total alkalinity; SWS, sea water scale; AB, atmosphere balanced seawater.

replication. The experimental chambers were designed originally by Kimura et al. (2011) and were constructed of sections of PVC pipe (volume, 180 mL) with eight holes (diameter, 10 mm) drilled in the side wall (Fig. 1). These holes and the bottom of the chambers were sealed with 80-μm mesh nylon to allow water to infiltrate the chambers. The chambers were submerged in 300-mL plastic bottles connected to peristaltic pump tubing that periodically pumped the pCO₂-controlled seawater into the plastic bottle (Fig. 1). The pCO₂-controlled seawater was maintained at a flow rate of ~10 mL min⁻¹ in the bottles. The bottles and the experimental chamber were placed in a ~20 °C water bath, and the larvae were reared until the veliger stage with completed larval shell for 3 days. After 3 days, all larvae were fixed in 50% ethanol, and mortality and malformation rates were calculated under an inverted microscope. Malformed larva was defined as an individual which was not capable of taking their soft body parts in the shell completely (Fig. S2). Maximum larval shell length of 20 surviving larvae, which were selected randomly from each chamber, was also measured using a monitor and video camera system (Nikon DIGITAL SIGHT DS-U3; NIKON CORPORATION, Minato-ku, Tokyo, Japan) with an image analyzer (NIS-Elements D 4.10.00; NIKON CORPORATION, Minato-ku, Tokyo, Japan) connected to the inverted microscope (Nikon EXLIPSE Ti-U; NIKON CORPORATION, Minato-ku, Tokyo, Japan).

Exp. II was carried out at the Miyako laboratory on 17–21 November 2014 (Table 1). Eggs and sperm were fertilized in 20 °C UV-irradiated seawater and rinsed three times to remove excess sperm. The fertilized eggs were placed in a 2-L plastic bottle containing 450 (atmosphere-balanced seawater) or 780 μatm pCO₂ experimental seawater and kept in an incubation room at 20 °C. After the incubation, active and normally developed trochophore larvae were selected under a stereoscopic microscope and placed in experimental chambers with running seawater adjusted to constant treatment levels of 450 or 780 μatm pCO₂ or the fluctuating diurnal cycle treatments of 450 ± 80, 780 ± 200, and 780 ± 400 μatm pCO₂ at a density of 200 individuals per chamber (Table 1). The larvae were reared in the chambers until the veliger stage for ~3 days. Five experimental chambers were assigned to each treatment as replication. Other experimental conditions and procedures were similar to those described for Exp. I.

To clarify the relationships between level and duration of seawater pCO₂ to which the abalone were exposed and the effects on larval fitness, the effective cumulative partial pressure of CO₂ (ECPC), which is defined as the integrated value of seawater pCO₂ over a specific criterion value, was calculated from equation (1):

$$ECPC = \sum_{i=1}^n (P_i - \theta) \quad (1)$$

where P_i is the hourly pCO₂ value to which the animals were exposed (P_i values < θ were not added), and n is rearing time (h). The threshold pCO₂ level (θ) was defined as the pCO₂ value corresponding 1.1 of aragonite saturation state (Ω-aragonite) in seawater, which produced a serious negative effect on shell formation the abalone (see Results). In this study, the θ was provided as 1120 μatm pCO₂ for Exp. I in the Shigama laboratory and as 1215 μatm pCO₂ for Exp. II in the Miyako laboratory, which were estimated using the CO₂SYS computer program with values of targeted Ω-aragonite, total alkalinity (TA), temperature and salinity in each experimental seawater (Pierrot et al., 2006).

2.5. Seawater chemistry measurements

pCO₂ level and temperature in the seawater were logged every hour by the AICAL system. Water temperature in the seawater reservoirs was measured periodically during the experiments, and the temperature difference between the reservoir and the pCO₂ equilibration towers was ± 0.5 °C. Salinity of the seawater in the reservoir was also measured periodically using a refractometer (ATAGO S/Mill; Atago Co. Ltd., Tokyo, Japan). pH and carbonate saturation (Ω-calcite and Ω-aragonite) were calculated from measured values of pCO₂, temperature, salinity, and total alkalinity (TA) using the CO₂SYS computer program (Pierrot et al., 2006). Mean TA values of seawater pumped into Shigama laboratory, which were measured by Kimura et al. (2011) on 8–12 December 2008 (described in Table 1 of Kimura et al., 2011), were used for the calculations in the Exp. I. The TA value for Exp. II conducted at the Miyako laboratory was measured in seawater collected from the water reservoir. The bottles with the water samples were sealed with caps and stored at ~5 °C for 1–2 months. TA was measured following the method of Ono et al. (1998). pH in the seawater reservoirs and experimental chambers was measured every hour with a handheld pH meter (Mettler Toledo SevenGo Portable pH Meter; Mettler-Toledo International Inc., Columbus, Ohio, USA) for the first 18 consecutive hours during Exp. I to evaluate the pCO₂ response time lag between them.

2.6. Statistical analysis

Mortality, and malformation rates as well as larval shell length were compared by one-way analysis of variance (ANOVA) with the pCO₂

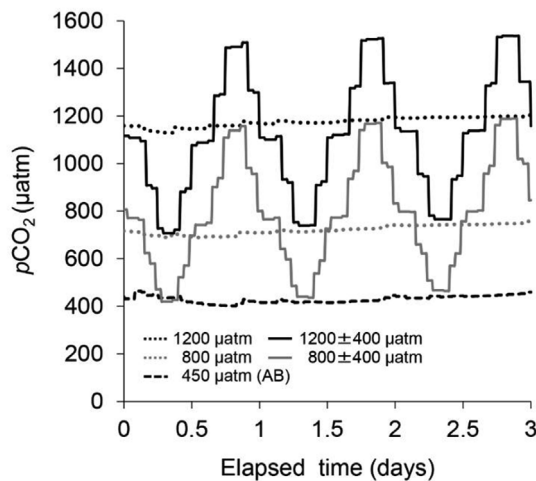


Fig. 2. Changes in partial pressure of CO_2 ($p\text{CO}_2$) of experimental seawater during the first flowing water experiment (Exp. I; 21–24 December 2010 in the Shiogama laboratory). Lines represent the values monitored by the AICAL system every hour. AB, atmosphere balanced seawater.

treatment as the fixed factor. When p -values under 0.05 were detected, Tukey–Kramer multiple comparison test were used to determine differences between the treatments. Homoscedasticity of the data was assessed using Bartlett's test. Percentage data were arcsine-transformed before statistical analyses. The significance of the regression coefficient was tested with the t -test. All statistical analyses were carried out with JMP ver. 6.0.2 (SAS Institute, Cary, NC, USA) or BellCurve for Excel ver. 2.11 (Social Survey Research Information Co., Ltd., Tokyo, Japan).

3. Results

3.1. Treatment conditions

The chemical and physical conditions used in the experiments are summarized in Table 2. In Exp. I, $p\text{CO}_2$ in all $p\text{CO}_2$ -constant treatments was maintained within 90 μatm of the target value (Fig. 2), and the $p\text{CO}_2$ values were distinguishable and clearly separated between the treatments. Seawater $p\text{CO}_2$ in the 800 ± 400 and 1200 ± 400 μatm $p\text{CO}_2$ treatments changed in the ranges of 420.3–1189.0 and 707.1–1537.1 μatm , respectively (Fig. 2, Table 2). The gap in pH between the seawater reservoir and the experimental chamber at each time point was within 0.06 for all $p\text{CO}_2$ treatments (Fig. S3), indicating no considerable response time lag in water exchange between them.

In Exp. II, $p\text{CO}_2$ was maintained within 35 μatm of the target value in all of the $p\text{CO}_2$ -constant treatments (Fig. 3, Table 2) and was clearly separated between treatments. The $p\text{CO}_2$ values of the experimental seawater in the 450 ± 80 , 780 ± 200 , and 780 ± 400 μatm $p\text{CO}_2$ treatments changed in the ranges of 409.3–573.6, 583.8–1035.0, and 490.6–1243.9 μatm , respectively (Fig. 3, Table 2).

3.2. Effects of cyclical fluctuations in seawater $p\text{CO}_2$ on larval survival and malformation rates and shell length

Mortality and malformation rates of larval *H. discus hannai* in Exp. I tended to increase, and their shells became smaller as $p\text{CO}_2$ was increased (Fig. 4). Significant differences were detected among the treatments in mortality rate, malformation rate, and larval shell length (mortality rate: ANOVA, $n = 3$, $F_{4,10} = 6.41$, $p = .008$, malformation rate: ANOVA, $n = 3$, $F_{4,10} = 12.72$, $p < .001$, larval shell length: ANOVA, $n = 3$, $F_{4,10} = 32.04$, $p < .001$). No differences in larval mortality or malformation rates or shell size were detected among the 450, 800, and 800 ± 400 μatm $p\text{CO}_2$ treatments in Exp. I (Tukey–Kramer test, $n = 3$, $p > .05$), although larvae in the

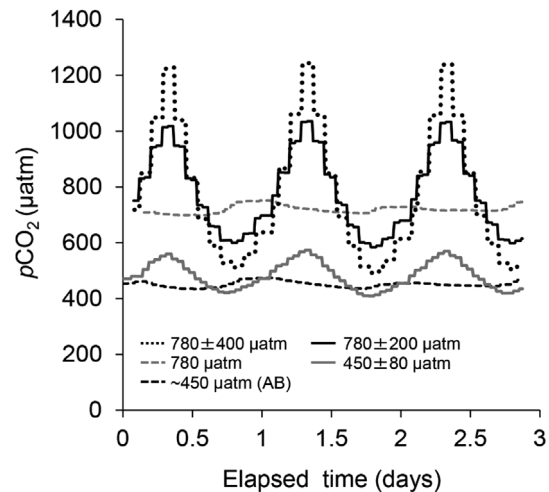


Fig. 3. Changes in partial pressure of CO_2 ($p\text{CO}_2$) of the experimental seawater during the second flowing water experiment (Exp. II; 18–21 November 2014 in the Miyako laboratory). Lines represent the values monitored by the AICAL system every hour. AB, atmosphere balanced seawater.

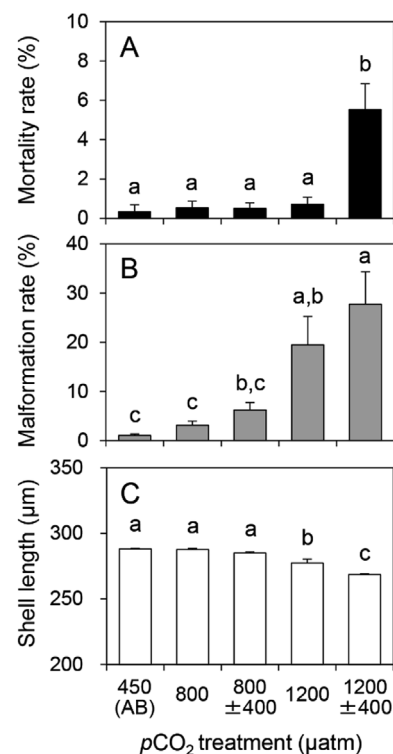


Fig. 4. Mortality rates (A), malformation rates (B), and shell length (C) of larval *Haliotis discus hannai* in the partial pressure of CO_2 ($p\text{CO}_2$) treatments 72 h after initiating Exp. I. Same letters indicate no significant difference among the groups (Tukey–Kramer test, $p > .05$). Each bar represents mean with standard error ($n = 3$). AB, atmosphere balanced seawater.

800 ± 400 μatm $p\text{CO}_2$ treatment showed a slightly higher malformation rate and shorter shells than those in the 450 and 800 μatm $p\text{CO}_2$ treatments (Fig. 4). In contrast, malformation rates in the 1200 and the 1200 ± 400 μatm $p\text{CO}_2$ treatments were significantly higher than those in the 450 and the 800 μatm $p\text{CO}_2$ treatments (Tukey–Kramer test, $n = 3$, $p < .05$, Fig. 4B). Larval shells were also significantly shorter in the 1200 and 1200 ± 400 μatm $p\text{CO}_2$ treatments than those in the 450, 800, and 800 ± 400 μatm $p\text{CO}_2$ treatments (Fig. 4C). Larval mortality rate in the 1200 ± 400 μatm $p\text{CO}_2$ treatment was significantly higher than that in the other $p\text{CO}_2$ treatments (Tukey–Kramer

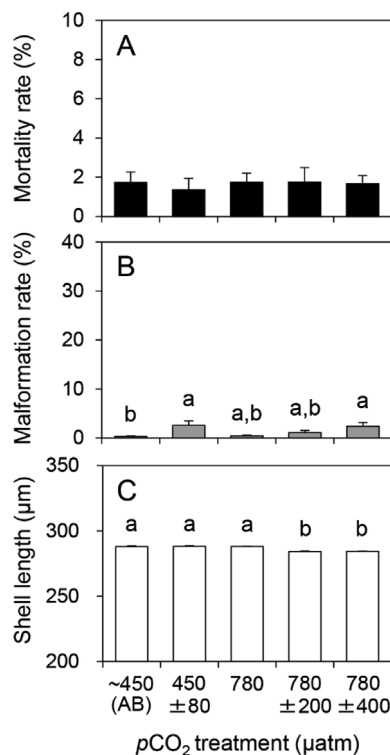


Fig. 5. Larval mortality rates (A), malformation rates (B), and shell length (C) of *Haliotis discus hannai* in the partial pressure of CO_2 ($p\text{CO}_2$) treatments 72 h after initiating Exp. II. Same letters indicate no significant difference among the groups (Tukey–Kramer test, $p > .05$). Each bar represents mean with standard error ($n = 5$). AB, atmosphere balanced seawater.

test, $n = 3$, $p < .05$, Fig. 4A). For malformation rate and larval shell length in Exp. II, significant differences were detected among the treatments (malformation rate: ANOVA, $n = 5$, $F_{4,20} = 4.40$, $p = .010$, larval shell length: ANOVA, $F_{4,20} = 11.39$, $p < .001$, Fig. 5). Larval shells were significantly shorter in the 780 \pm 200 and 780 \pm 400 μatm $p\text{CO}_2$ treatments than those in the other treatments in Exp. II (Tukey–Kramer test, $n = 5$, $p < .05$, Fig. 5C). Malformation rate was significantly higher in the 450 \pm 80 and the 780 \pm 400 μatm $p\text{CO}_2$ treatments than in the 450 μatm $p\text{CO}_2$ treatments (Tukey–Kramer test, $n = 5$, $p < .05$, Fig. 5B). Although some significant differences were detected, differences in larval mortality, malformation rates or shell length of *H. discus hannai* among the treatments in Exp. I were relatively small compared with those in Exp. I.

Malformation rate in Exps. I and II increased exponentially with decreasing of aragonite saturation state in the experimental seawater (Fig. 6); malformation rate greatly increased in the individuals experienced nearly unsaturated and/or unsaturated aragonite conditions (Ω -aragonite ≤ 1.1), and there were no large differences in the rate between the larvae kept in aragonite-saturated seawater (Ω -aragonite > 1.1). Meanwhile, shell length of larval *H. discus hannai* declined logarithmically as the aragonite saturation state decreased (Fig. 6); shell length decreased markedly in larvae maintained in nearly unsaturated and/or unsaturated aragonite conditions (Ω -aragonite ≤ 1.1), whereas little difference in shell length was observed between larvae held in aragonite-saturated seawater (Ω -aragonite > 1.1).

Based on the results of the Exps. I and II showing that the seawater with Ω -aragonite ≤ 1.1 had negative impact on larval shell formation of *H. discus hannai*, we defined the threshold level (θ) as the $p\text{CO}_2$ corresponding to 1.1 of aragonite saturation state in the seawater. The ECPC was calculated using equation (1) with the threshold value (θ) set to 1120 and 1215 μatm $p\text{CO}_2$ for Exp. I and II, respectively. The relationships between larval fitness (mortality and malformation rates as well as larval shell length) and the ECPC in Exps. I and II were shown in

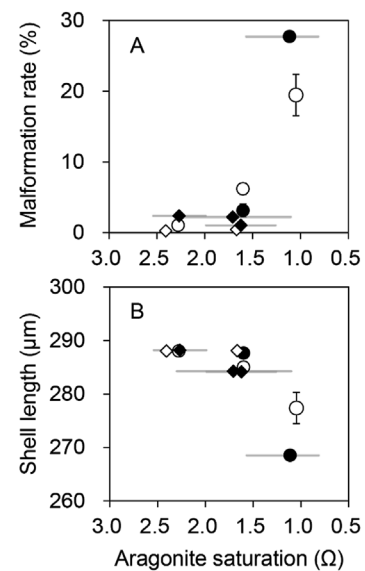


Fig. 6. Relationships between malformation rate (A) and shell length (B) of larval *Haliotis discus hannai* 72 h after initiating the flowing water experiments (Exps. I and II) and aragonite saturation state (Ω -aragonite) in the experimental seawater. Circular and rhombic symbols represent Exp. I and Exp. II data, respectively. White- and black-colored symbols show mean value of malformation rate/larval shell length (Exp. I; $n = 3$ and Exp. II; $n = 5$) in treatments with constant and cyclically fluctuating partial pressure of CO_2 ($p\text{CO}_2$) in the $p\text{CO}_2$ treatments, respectively. Each vertical and horizontal bar represents standard error in malformation rate/shell length and the fluctuating range of Ω -aragonite, respectively.

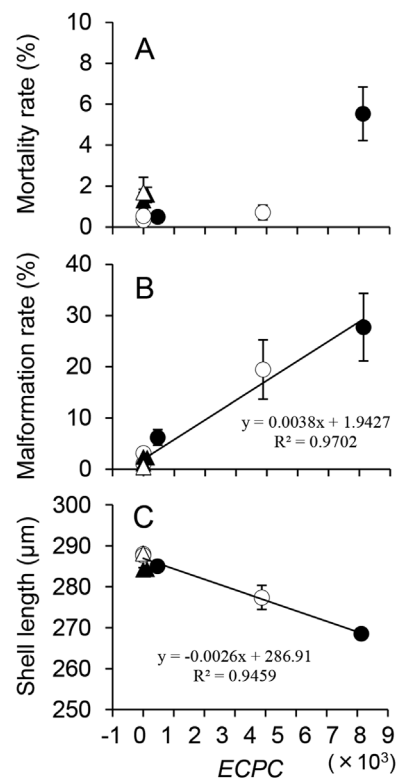


Fig. 7. Relationships between larval mortality rates (A), malformation rates (B), and shell length (C) of *Haliotis discus hannai* 72 h after initiating the flowing water experiments (Exps. I and II) and the effective cumulative partial pressure of CO_2 (ECPC). Circular and triangular symbols represent mean value of mortality rate, malformation rates, or shell length (Exp. I; $n = 3$ and Exp. II; $n = 5$) in Exp. I and Exp. II, respectively. White- and black-colored symbols represent the results of the treatments with a constant and cyclically fluctuating partial pressure of CO_2 ($p\text{CO}_2$), respectively. Only significant regression lines are shown ($p < .05$). Each bar represents standard error.

Fig. 7. The ECPC have clear relationships with malformation rate and larval shell length (Fig. 7B, C), but showed no association with mortality rate.

4. Discussion

In this study, we found that the negative effects on survival, and larval shell formation of *H. discus hannai* tended to be greater with increasing $p\text{CO}_2$ in the experimental seawater, and then were further strengthened when $p\text{CO}_2$ fluctuated diurnally, particularly at $p\text{CO}_2 > 1100 \mu\text{atm}$.

Larval mortality and malformation rates as well as shell length in the $800 \pm 400 \mu\text{atm}$ treatment of Exp. I were not different from those in the 450 and $800 \mu\text{atm}$ $p\text{CO}_2$ treatments (Fig. 4). Additionally, no great differences were observed in these parameters during Exp. II covering a range of 409–1244 μatm $p\text{CO}_2$, regardless of whether seawater $p\text{CO}_2$ fluctuated or not (Fig. 5). The results indicate that diurnal fluctuations in seawater $p\text{CO}_2$ within $800 \mu\text{atm}$ ($\pm 400 \mu\text{atm}$ $p\text{CO}_2$) have no serious effect on early development of larval *H. discus hannai*. In contrast, significant differences in larval mortality and malformation rates as well as shell length were observed between the 800 ± 400 and $1200 \pm 400 \mu\text{atm}$ $p\text{CO}_2$ treatments in Exp. I, despite the similar magnitude of $p\text{CO}_2$ fluctuations. These results suggest that there is a threshold $p\text{CO}_2$ level for generating detrimental effects on larval fitness, and that diurnal $p\text{CO}_2$ fluctuations within a subthreshold range do not seriously effect early development and larval shell formation of *H. discus hannai*. In addition, great differences in mortality, malformation rates, and larval shell length were also detected between the 1200 and $1200 \pm 400 \mu\text{atm}$ $p\text{CO}_2$ treatments in the Exp. I, indicating that $p\text{CO}_2$ fluctuations can produce greater negative effects on abalone when above the threshold level than those observed under static $p\text{CO}_2$ conditions.

Larval shell length decreased significantly in the 1200 and the $1200 \pm 400 \mu\text{atm}$ $p\text{CO}_2$ treatments (Fig. 4), probably owing to the long-term exposure to $p\text{CO}_2 > 1000 \mu\text{atm}$ (Fig. 2), whereas shell length in treatments $\leq 1000 \mu\text{atm}$ $p\text{CO}_2$ decreased gradually with increasing seawater $p\text{CO}_2$ (Fig. 4). The early calcification process of benthic mollusks responds strongly to increased $p\text{CO}_2$, decreased pH, CO_3^{2-} concentration, and CaCO_3 saturation state (Fabry et al., 2008) because calcification is mediated by the weak acid distribution of CO_2 and acid–base regulation across the body compartmental barriers (Pörtner, 2012; Wittmann and Pörtner, 2013). Carbonate precipitation is set by the saturation of calcium carbonate at the calcification sites (Pörtner, 2008), and saturation is affected by the calcium level set in various internal compartments. Larval bivalve and gastropod shells consist of aragonite or amorphous CaCO_3 (Iwata, 1978; Weiss et al., 2002); thus, the downsizing and malformation of the larval *H. discus hannai* shell found in this study may be related to the aragonite saturation state in the experimental seawater. Shell length of larval *H. discus hannai* decreased gradually with increasing seawater $p\text{CO}_2$ under a saturated aragonite state (Fig. 6B, $\Omega\text{-aragonite} > 1.1$), and great downsizing was observed in the 1200 and the $1200 \pm 400 \mu\text{atm}$ $p\text{CO}_2$ treatments, which were nearly unsaturated or unsaturated aragonite states (Fig. 6B, $\Omega\text{-aragonite} \leq 1.1$). Similarly, malformation rate was low for larvae kept in aragonite-saturated condition (Fig. 6A, $\Omega\text{-aragonite} > 1.1$), but markedly increased in those held in nearly unsaturated or unsaturated aragonite condition (Fig. 6A, $\Omega\text{-aragonite} \leq 1.1$). A similar relationship between larval shell size and aragonite saturation state in seawater was reported for the horned turban, *Turbo cornutus*, which also inhabits coastal rocky habitats as a dominant grazer (Onitsuka et al., 2014). *T. cornutus* veliger shell length decreased gradually as seawater $p\text{CO}_2$ was increased under an aragonite saturated condition ($\Omega\text{-aragonite} > 1.04$) but decreased significantly in nearly unsaturated and/or unsaturated aragonite conditions ($\Omega\text{-aragonite} \leq 1.04$). However, the relationship may not be universal for all marine calcifiers. Ries et al. (2009) showed that changes in calcification rates in response to increasing $p\text{CO}_2$ vary

greatly among taxa and species. These different response patterns may be affected by combinations of various factors, such as the ability to regulate pH at the calcification site, the extent of organic-layer coverage of the external shell, biomineral solubility, and whether the organism can photosynthesize (Ries et al., 2009). Further studies are needed to understand how $p\text{CO}_2$ changes in ambient seawater affect shell formation/conservation and the internal chemical environment of marine calcifiers.

Kimura et al. (2011) demonstrated that constant seawater $p\text{CO}_2 < 1100 \mu\text{atm}$ has no negative effects on fertilization, malformation rate, survival, or shell size in larval *H. discus hannai*, and that 1000–1600 μatm is a critical $p\text{CO}_2$ range for *H. discus hannai*. Similarly, we found no differences in larval mortality or malformation rates as well as shell length at $< 1000 \mu\text{atm}$ $p\text{CO}_2$ in Exp. I (the 450 and the $800 \mu\text{atm}$ $p\text{CO}_2$ treatments), whereas a significantly higher malformation rate and smaller larval shells were detected in the $1200 \mu\text{atm}$ $p\text{CO}_2$ treatment (Fig. 4). Additionally, larvae in the $800 \pm 400 \mu\text{atm}$ $p\text{CO}_2$ treatment in Exp. I and the $780 \pm 400 \mu\text{atm}$ $p\text{CO}_2$ treatment in Exp. II, which involved short-term exposure to $p\text{CO}_2 > 1000 \mu\text{atm}$, showed only slight decreases in shell length (Figs. 4 and 5) and increased malformation rate. These results suggest that the critical $p\text{CO}_2$ level producing negative effects on larval abalone is around 1000–1200 μatm . From the relationship between aragonite saturation state and malformation rate/larval shell length (Fig. 6), detrimental effects on larval shell formation were observed around 1.1 of the aragonite saturation state, which corresponded to 1000–1300 μatm $p\text{CO}_2$ in the experimental seawaters. From these results, therefore, it is assumed that the $p\text{CO}_2$ corresponding to 1.1 of the aragonite saturation state in the seawater is a threshold level producing serious negative effects on the abalone in early life. A definite relationship between malformation rate/larval shell length and the ECPC (Fig. 7) also justify the threshold level, and then supports our hypothesis that the intensity and time of exposure to seawater $p\text{CO}_2$ over a particular threshold level is a critical factor determining the negative effects of $p\text{CO}_2$ on early development and larval shell formation of *H. discus hannai*.

Early life survival is thought to be a key factor determining subsequent recruitment and population dynamics in many benthic marine animals (Gosselin and Qian, 1997; Hunt and Scheibling, 1997). Downsized and malformed larval abalone shells produced in an acidified ocean can be vulnerable to physical and biological factors, such as disturbance and predation, consequently, will result in negative effects on survival and recruitment of the abalone. Moreover, these negative effects could be strengthened by diurnal fluctuations in seawater $p\text{CO}_2$, particularly those $> 1000 \mu\text{atm}$ (Figs. 4 and 5). Thus, acidified oceans with diurnally fluctuating $p\text{CO}_2$ due to progressive OA could have strong negative effects on abalone, and these effects will occur sooner than expected based on previous experimental results under $p\text{CO}_2$ -static conditions. Consequently, decreases in early survival would pose a danger to conservation and sustainable use of natural abalone stocks in the future.

This study found that there is a threshold $p\text{CO}_2$ level producing serious negative effects on larval *H. discus hannai*, and the threshold corresponds to 1.1 of the aragonite saturation state in the seawater. We demonstrated that diurnal fluctuations in seawater $p\text{CO}_2$ within $800 \mu\text{atm}$ ($\pm 400 \mu\text{atm}$ $p\text{CO}_2$) but below the threshold level had no significant effects on early development of *H. discus hannai*. In contrast, $p\text{CO}_2$ fluctuations could have added negative effects on abalone over the threshold. This study also showed that the negative effects of seawater with increased $p\text{CO}_2$ on larval abalone would be determined by intensity ($p\text{CO}_2$ level) and time of exposure to $p\text{CO}_2$ over the threshold level. These negative effects of increasing seawater $p\text{CO}_2$ with diurnal fluctuations on abalone will be complicated more by ocean warming, which is proceeding simultaneously with OA. Some studies have examined the combined effects of increased temperature and elevated $p\text{CO}_2$ on some calcifiers (e.g. Byrne et al., 2010, 2011; Findlay et al., 2010; Sheppard Brennard et al., 2010; Ericson et al., 2012; Landes and

Zimmer, 2012; Thiagarajan and Ko, 2012) and showed that increased temperature has a synergistic (Findlay et al., 2010; Ericson et al., 2012) or compensating/mitigating effect (Sheppard Brennand et al., 2010; Byrne et al., 2011) with the effects of elevated $p\text{CO}_2$, suggesting that the combined effects may be species-specific in marine organisms (Byrne et al., 2011). Furthermore, the threshold to CO_2 may be affected by not only temperature but also the other factors such as dissolved oxygen level in ambient seawater (e.g. Sui et al., 2016).

Environmental water quality, such as $p\text{CO}_2$, pH, and carbonate saturation state, in coastal areas inhabited by the majority of ecologically and economically important marine organisms can change spatiotemporally owing to upwelling (Feely et al., 2008; Hofmann et al., 2011), river discharge (Borges and Frankignoulle, 1999), and eutrophication (Cai et al., 2011), as well as besides OA. Furthermore, the magnitude of the diurnal $p\text{CO}_2$ variations in the ocean produced by photosynthesis and respiration will also vary depending on biological activity in each area and season. Therefore, the effects of OA on coastal marine organisms will vary according to location, depth, habitat, season, and year (e.g. Hofmann et al., 2011; Buapet et al., 2013). Limited information is available about daily and long-term changes in water quality, such as $p\text{CO}_2$, TA, dissolved inorganic carbon, pH, salinity, and temperature, in coastal waters (e.g. Borges and Frankignoulle, 1999; Semesi et al., 2009; Hofmann et al., 2011; Yu et al., 2011; Price et al., 2012). A better understanding of chemical and biological characteristics in local waters and an examination of the combined effects of multiple stressors related to climate is needed to accurately assess changes in local marine organisms and communities caused by future warming and OA.

5. Conclusion

This study showed that seawater with highly elevated $p\text{CO}_2$ has negative effects on survival and shell formation of larval *H. discus hannai*, and that there is a $p\text{CO}_2$ threshold producing serious negative effects. It was also suggested that the $p\text{CO}_2$ threshold would be associated with Ω -aragonite in the seawater. Our experiments demonstrated that diurnal fluctuations in seawater $p\text{CO}_2$ within $800 \mu\text{atm}$ ($\pm 400 \mu\text{atm } p\text{CO}_2$) below the threshold level had no significant effects on early development of *H. discus hannai*, but could have added negative effects on the abalone over the threshold. Clear relationships between abalone fitness and the integrated $p\text{CO}_2$ value over the threshold, which were found in this study, suggested that development and shell formation of larval abalone can be affected by intensity and time of exposure to $p\text{CO}_2$ over the threshold. Acidified oceans with diurnally fluctuating $p\text{CO}_2$ due to progressive OA could have strong negative effects on abalone, and these effects will occur sooner than expected based on previous experimental results under $p\text{CO}_2$ -static conditions.

Acknowledgments

We thank Mr. S. Saito helped maintenance of the AICAL system and abalone rearing. This study was supported by JSPS KAKENHI [Grant Number 23241017, 26220102].

Appendix A. Supplementary data

Supplementary data related to this article can be found at <http://dx.doi.org/10.1016/j.marenvres.2017.12.015>.

References

Borges, A.V., Frankignoulle, M., 1999. Daily and seasonal variations of the partial pressure of CO_2 in surface seawater along Belgian and southern Dutch coastal areas. *J. Mar. Syst.* 19, 251–266.
Buapet, P., Gullstrom, M., Bjork, M., 2013. Photosynthetic activity of seagrasses and macroalgae in temperate shallow waters can alter seawater pH and total inorganic carbon content at the scale of a coastal embayment. *Mar. Freshw. Res.* 64,

1040–1048.
Byrne, M., Ho, M., Wong, E., Soars, N.A., Selvakumaraswamy, P., Shepard-Brennand, H., Dworjanyn, S.A., Davis, A.R., 2011. Unshelled abalone and corrupted urchins: development of marine calcifiers in a changing ocean. *Proc. R. Soc. B* 278, 2376–2383.
Byrne, M., Soars, N.A., Ho, M.A., Wong, E., McElroy, D., Selvakumaraswamy, P., Dworjanyn, S.A., Davis, A.R., 2010. Fertilization in a suite of coastal marine invertebrates from SE Australia is robust to near-future ocean warming and acidification. *Mar. Biol.* 157, 2061–2069.
Cai, W.J., Hu, X.P., Huang, W.J., Murrell, M.C., Lehrter, J.C., Lohrenz, S.E., Chou, W.C., Zhai, W.D., Hollibaugh, J.T., Wang, Y.C., Zhao, P.S., Guo, X.H., Gundersen, K., Dai, M.H., Gong, G.C., 2011. Acidification of subsurface coastal waters enhanced by eutrophication. *Nat. Geosci.* 4, 766–770.
Caldeira, K., Wickett, M.E., 2003. Anthropogenic carbon and ocean pH. *Nature* 425, 365.
Clark, H.R., Gobler, C.J., 2016. Diurnal fluctuations in CO_2 and dissolved oxygen concentrations do not provide a refuge from hypoxia and acidification for early-life-stage bivalves. *Mar. Ecol. Prog. Ser.* 558, 1–14.
Cornwall, C.E., Hepburn, C.D., McGraw, C.M., Currie, K.I., Pilditch, C.A., Hunter, K.A., Boyd, P.W., Hurd, C.L., 2013. Diurnal fluctuations in seawater pH influence the response of a calcifying macroalga to ocean acidification. *Proc. R. Soc. B* 280, 20132201.
Crim, R.N., Sunday, J.M., Harley, C.D.G., 2011. Elevated seawater CO_2 concentrations impair larval development and reduce larval survival in endangered northern abalone (*Haliotis kamtschatkana*). *J. Exp. Mar. Biol. Ecol.* 400, 272–277.
Delille, B., Borges, A.V., Delille, D., 2009. Influence of giant kelp beds (*Macrocystis pyrifera*) on diel cycles of $p\text{CO}_2$ and DIC in the Sub-Antarctic coastal area. *Estuar. Coast Shelf Sci.* 81, 114–122.
Doo, S.S., Dworjanyn, S.A., Foo, S.A., Soars, N.A., Byrne, M., 2012. Impacts of ocean acidification on development of the meroplanktonic larval stage of the sea urchin *Centrostephanus rodgersii*. *ICES J. Mar. Sci.* 69, 460–464.
Ericson, J.A., Ho, M.A., Miskelly, A., King, C.K., Virtue, P., Tilbrook, B., Byrne, M., 2012. Combined effects of two ocean change stressors, warming and acidification, on fertilization and early development of the Antarctic echinoid *Sterechninus neumayeri*. *Polar Biol.* 35, 1027–1034.
Fabry, V.J., Seibel, B.A., Feely, R.A., Orr, J.C., 2008. Impacts of ocean acidification on marine fauna and ecosystem processes. *ICES J. Mar. Sci.* 65, 414–432.
Feely, R.A., Sabine, C.L., Hernandez-Ayon, J.M., Ianson, D., Hales, B., 2008. Evidence for upwelling of corrosive “acidified” water onto the continental shelf. *Science* 320, 1490–1492.
Feely, R.A., Sabine, C.L., Lee, K., Berelson, W., Kleypas, J., Fabry, V.J., Millero, F.J., 2004. Impact of anthropogenic CO_2 on the CaCO_3 system in the oceans. *Science* 305, 362–366.
Findlay, H.S., Kendall, M.A., Spicer, J.I., Widdicombe, S., 2010. Post-larval development of two intertidal barnacles at elevated CO_2 and temperature. *Mar. Biol.* 157, 725–735.
Fujita, K., Hikami, M., Suzuki, A., Kuroyanagi, A., Sakai, K., Kawahata, H., Nojiri, Y., 2011. Effects of ocean acidification on calcification of symbiont-bearing reef foraminifers. *Biogeosciences* 8, 2089–2098.
Gattuso, J.P., Buddemeier, R.W., 2000. Ocean biogeochemistry-calcification and CO_2 . *Nature* 407, 311–313.
Gazeau, F., Quiblier, C., Jansen, J.M., Gattuso, J.P., Middelburg, J.J., Heip, C.H.R., 2007. Impact of elevated CO_2 on shellfish calcification. *Geophys. Res. Lett.* 34, L07603.
Gosselin, L.A., Qian, P.Y., 1997. Juvenile mortality in benthic marine invertebrates. *Mar. Ecol. Prog. Ser.* 146, 265–282.
Hofmann, G.E., Smith, J.E., Johnson, K.S., Send, U., Levin, L.A., Micheli, F., Paytan, A., Price, N.N., Peterson, B., Takeshita, Y., Matson, P.G., Crook, E.D., Kroeker, K.J., Gambi, M.C., Rivest, E.B., Frieder, C.A., Yu, P.C., Martz, T.R., 2011. High-frequency dynamics of ocean pH: a multi-ecosystem comparison. *Plos One* 6, e28983.
Hunt, H.L., Scheiblich, R.E., 1997. Role of early post-settlement mortality in recruitment of benthic marine invertebrates. *Mar. Ecol. Prog. Ser.* 155, 269–301.
Iwata, K., 1978. A study on calcification of the protoconch of *Haliotis discus hannai* Ito, (Archaeogastropoda). *Earth Sci.* 32, 51–57 (Japanese with English abstract).
Jarrold, M.D., Humphrey, C., McCormick, M.I., Munday, P.L., 2017. Diel CO_2 cycles reduce severity of behavioural abnormalities in coral reef fish under ocean acidification. *Sci. Rep.* 7, 10153.
Kimura, R., Takami, H., Ono, T., Onitsuka, T., Nojiri, Y., 2011. Effects of elevated $p\text{CO}_2$ on the early development of the commercially important gastropod, Ezo abalone *Haliotis discus hannai*. *Fish. Oceanogr.* 20, 357–366.
Kokubo, S., 1962. Marine biology, Suisangaku Zenshu 11. Kouseisha Kouseikaku Co., Ltd., Tokyo (In Japanese).
Kurihara, H., 2008. Effects of CO_2 -driven ocean acidification on the early developmental stages of invertebrates. *Mar. Ecol. Prog. Ser.* 373, 275–284.
Landes, A., Zimmer, M., 2012. Acidification and warming affect both a calcifying predator and prey, but not their interaction. *Mar. Ecol. Prog. Ser.* 450, 1–10.
Michaelidis, B., Ouzounis, C., Paleras, A., Pörtner, H.O., 2005. Effects of long-term moderate hypercapnia on acid-base balance and growth rate in marine mussels *Mytilus galloprovincialis*. *Mar. Ecol. Prog. Ser.* 293, 109–118.
Onitsuka, T., Kimura, R., Ono, T., Takami, H., Nojiri, Y., 2014. Effects of ocean acidification on the early developmental stages of the horned turban, *Turbo cornutus*. *Mar. Biol.* 161, 1127–1138.
Ono, T., Yasuda, I., Narita, H., Tsunogai, S., 1998. Chemical alternation of waters in the Kuroshio/Oyashio interfrontal zone. *J. Oceanogr.* 54, 681–694.
Parker, L.M., Ross, P.M., O'Connor, W.A., 2009. The effect of ocean acidification and temperature on the fertilization and embryonic development of the Sydney rock oyster *Saccostrea glomerata* (Gould 1850). *Global Change Biol.* 15, 2123–2136.
Pierrot, D., Lewis, E., Wallace, D.W.R., 2006. MS Excel Program Developed for CO_2 System Calculations. ORNL/CDIAC-105a. Carbon Dioxide Information Analysis

- Center, Oak Ridge National Laboratory, U.S. Department of Energy, Oak Ridge, Tennessee.
- Pörtner, H.O., 2008. Ecosystem effects of ocean acidification in times of ocean warming: a physiologist's view. *Mar. Ecol. Prog. Ser.* 373, 203–217.
- Pörtner, H.O., 2012. Integrating climate-related stressor effects on marine organisms: unifying principles linking molecule to ecosystem-level changes. *Mar. Ecol. Prog. Ser.* 470, 273–290.
- Price, N.N., Martz, T.R., Brainard, R.E., Smith, J.E., 2012. Diel variability in seawater pH relates to calcification and benthic community structure on coral reefs. *PLoS One* 7, e43843.
- Riebesell, U., Zondervan, I., Rost, B., Tortell, P.D., Zeebe, R.E., Morel, F.M.M., 2000. Reduced calcification of marine plankton in response to increased atmospheric CO₂. *Nature* 407, 364–367.
- Ries, J.B., Cohen, A.L., McCorkle, D.C., 2009. Marine calcifiers exhibit mixed responses to CO₂-induced ocean acidification. *Geology* 37, 1131–1134.
- Semesi, I.S., Beer, S., Bjork, M., 2009. Seagrass photosynthesis controls rates of calcification and photosynthesis of calcareous macroalgae in a tropical seagrass meadow. *Mar. Ecol. Prog. Ser.* 382, 41–47.
- Sheppard Brennan, H., Soars, N., Dworjanyn, S.A., Davis, A.R., Byrne, M., 2010. Impact of ocean warming and ocean acidification on larval development and calcification in the sea urchin *Tripneustes gratilla*. *PLoS One* 5, e11372.
- Shirayama, Y., Thornton, H., 2005. Effect of increased atmospheric CO₂ on shallow water marine benthos. *J. Geophys. Res. Oceans* 110, C09S08.
- Sui, Y.M., Kong, H., Huang, X.Z., Dupont, S., Hu, M.H., Storch, D., Pörtner, H.O., Lu, W.Q., Wang, Y.J., 2016. Combined effects of short-term exposure to elevated CO₂ and decreased O₂ on the physiology and energy budget of the thick shell mussel *Mytilus coruscus*. *Chemosphere* 155, 207–216.
- Suwa, R., Nojiri, Y., Ono, T., Shirayama, Y., 2013. Effects of low pCO₂ conditions on sea urchin larval size. *Mar. Ecol.* 34, 443–450.
- Tahil, A.S., Dy, D.T., 2016. Effects of reduced pH on the early larval development of hatchery-reared Donkey's ear abalone, *Haliotis asinina* (Linnaeus 1758). *Aquaculture* 459, 137–142.
- Takami, H., Oshino, A., Sasaki, R., Fukazawa, H., Kawamura, T., 2006. Age determination and estimation of larval period in field caught abalone (*Haliotis discus hannai* Ino 1953) larvae and newly metamorphosed post-larvae by counts of radular teeth rows. *J. Exp. Mar. Biol. Ecol.* 328, 289–301.
- Talmage, S.C., Gobler, C.J., 2009. The effects of elevated carbon dioxide concentrations on the metamorphosis, size, and survival of larval hard clams (*Mercenaria mercenaria*), bay scallops (*Argopecten irradians*), and Eastern oysters (*Crassostrea virginica*). *Limnol. Oceanogr.* 54, 2072–2080.
- Talmage, S.C., Gobler, C.J., 2011. Effects of elevated temperature and carbon dioxide on the growth and survival of larvae and juveniles of three species of northwest Atlantic bivalves. *PLoS One* 6, e26941.
- Thiyagarajan, V., Ko, G.W.K., 2012. Larval growth response of the Portuguese oyster (*Crassostrea angulata*) to multiple climate change stressors. *Aquaculture* 370, 90–95.
- Uki, N., Kikuchi, S., 1984. Regulation of maturation and spawning of an abalone, *Haliotis* (Gastropoda) by external environmental factors. *Aquaculture* 39, 247–261.
- Van Colen, C., Debusschere, E., Braeckman, U., Van Gansbeke, D., Vincx, M., 2012. The early life history of the clam *Macoma balthica* in a high CO₂ world. *PLoS One* 7, e44655.
- Watson, S.A., Peck, L.S., Tyler, P.A., Southgate, P.C., Tan, K.S., Day, R.W., Morley, S.A., 2012. Marine invertebrate skeleton size varies with latitude, temperature and carbonate saturation: implications for global change and ocean acidification. *Global Change Biol.* 18, 3026–3038.
- Weiss, I.M., Tuross, N., Addadi, L., Weiner, S., 2002. Mollusc larval shell formation: amorphous calcium carbonate is a precursor phase for aragonite. *J. Exp. Zool.* 293, 478–491.
- Wittmann, A.C., Pörtner, H.O., 2013. Sensitivities of extant animal taxa to ocean acidification. *Nat. Clim. Change* 3, 995–1001.
- Yu, P.C., Matson, P.G., Martz, T.R., Hofmann, G.E., 2011. The ocean acidification seascape and its relationship to the performance of calcifying marine invertebrates: laboratory experiments on the development of urchin larvae framed by environmentally-relevant pCO₂/pH. *J. Exp. Mar. Biol. Ecol.* 400, 288–295.